Lattice QCD with an inhomogeneous magnetic field background

XQCD 2022, Trondheim, Norway

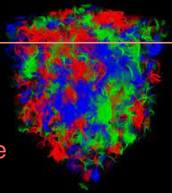

Dean Valois
dvalois@physik.uni-bielefeld.de

Gergely Endrődi   Bastian Brandt   Gergely Marko   Francesca Cuteri

July 27, 2022

Department of Physics
Bielefeld University

Outline

Strongly magnetized physical systems

STRONGLY MAGNETIZED PHYSICAL SYSTEMS

Early universe
$\sqrt{eB} \sim 1.5$ GeV

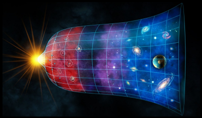

STRONGLY MAGNETIZED PHYSICAL SYSTEMS

Early universe

$\sqrt{eB} \sim 1.5$ GeV

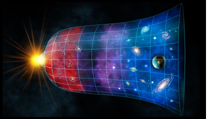

Heavy-ion collision

$\sqrt{eB} \sim 0.5$ GeV

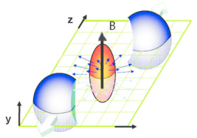

STRONGLY MAGNETIZED PHYSICAL SYSTEMS

Early universe

$\sqrt{eB} \sim 1.5$ GeV

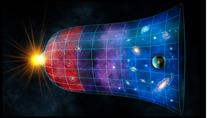

Heavy-ion collision

$\sqrt{eB} \sim 0.5$ GeV

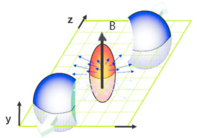

Neutron stars

$\sqrt{eB} \sim 1$ MeV

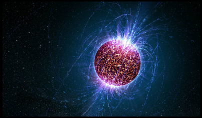

STRONGLY MAGNETIZED PHYSICAL SYSTEMS

Early universe

$\sqrt{eB} \sim 1.5$ GeV

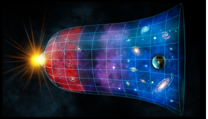

Heavy-ion collision

$\sqrt{eB} \sim 0.5$ GeV

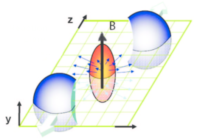

Neutron stars

$\sqrt{eB} \sim 1$ MeV

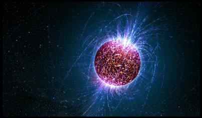

QCD vacuum

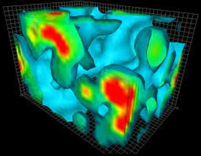

STRONGLY MAGNETIZED PHYSICAL SYSTEMS

Early universe

$\sqrt{eB} \sim 1.5$ GeV

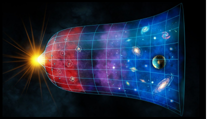

Heavy-ion collision

$\sqrt{eB} \sim 0.5$ GeV

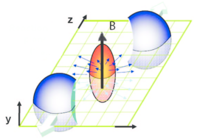

Neutron stars

$\sqrt{eB} \sim 1$ MeV

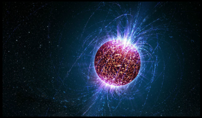

QCD vacuum

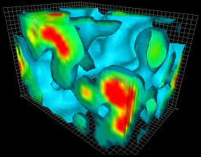

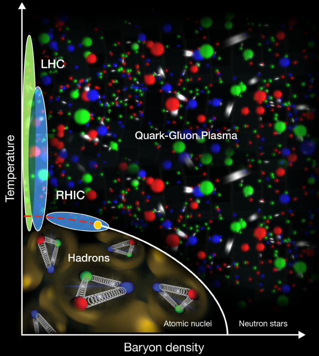

MAGNETIC FIELDS IN HEAVY-ION COLLISIONS

MAGNETIC FIELDS IN HEAVY-ION COLLISIONS

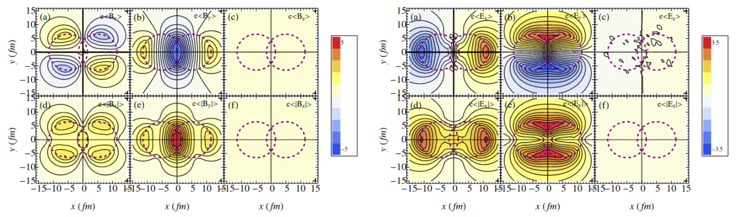

Figure 2: Spatial distributions of the electric (right) and magnetic (left) fields in the transverse plane for an impact parameter $b = 10$ fm Deng and Huang 2012.

MAGNETIC FIELDS IN HEAVY-ION COLLISIONS

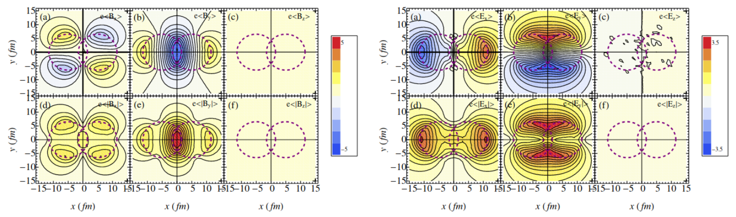

Figure 2: Spatial distributions of the electric (right) and magnetic (left) fields in the transverse plane for an impact parameter $b = 10$ fm Deng and Huang 2012.

Caveats:

- **B** and **E** are highly non-homogeneous.

MAGNETIC FIELDS IN HEAVY-ION COLLISIONS

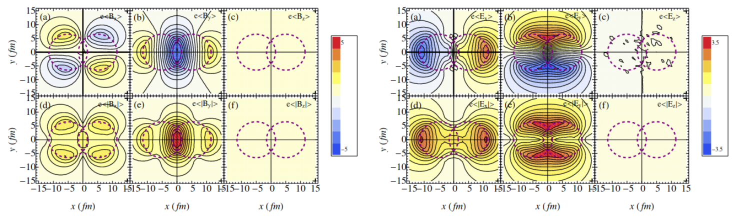

Figure 2: Spatial distributions of the electric (right) and magnetic (left) fields in the transverse plane for an impact parameter $b = 10$ fm Deng and Huang 2012.

Caveats:

- **B** and **E** are highly non-homogeneous.
- A real **E** leads to sign problem.

MAGNETIC FIELDS IN HEAVY-ION COLLISIONS

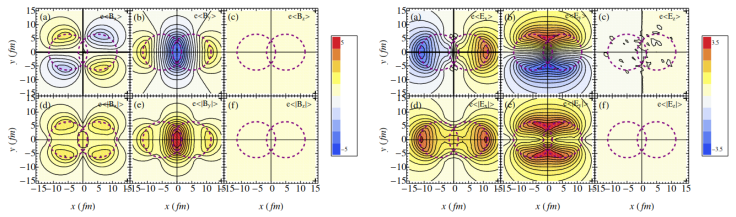

Figure 2: Spatial distributions of the electric (right) and magnetic (left) fields in the transverse plane for an impact parameter $b = 10$ fm Deng and Huang 2012.

Caveats:

- **B** and **E** are highly non-homogeneous.
- A real **E** leads to sign problem.
- No Minkoswki time evolution from Euclidean simulations.

Magnetic fields in heavy-ion collisions

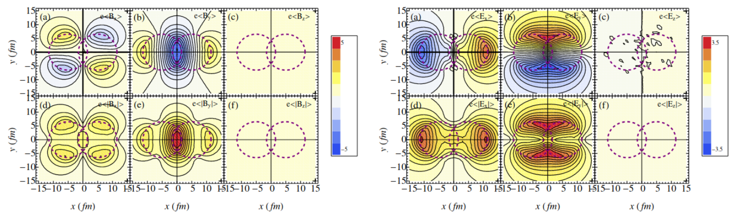

Figure 2: Spatial distributions of the electric (right) and magnetic (left) fields in the transverse plane for an impact parameter $b = 10$ fm Deng and Huang 2012.

Caveats:

- **B** and **E** are highly non-homogeneous.
- A real **E** leads to sign problem.
- No Minkoswki time evolution from Euclidean simulations.

What can we do?

Magnetic fields in heavy-ion collisions

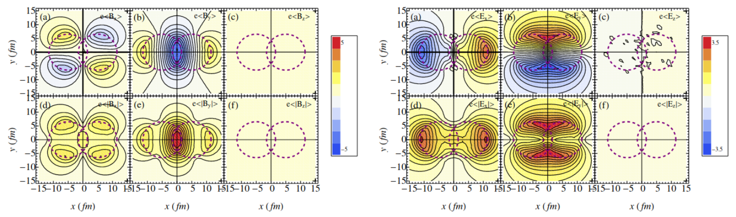

Figure 2: Spatial distributions of the electric (right) and magnetic (left) fields in the transverse plane for an impact parameter $b = 10$ fm Deng and Huang 2012.

Caveats:

- **B** and **E** are highly non-homogeneous.
- A real **E** leads to sign problem.
- No Minkoswki time evolution from Euclidean simulations.

What can we do?

$B(x)$ as background in lattice QCD!

Magnetic field on the lattice

UNIFORM MAGNETIC FIELD ON THE LATTICE

fermion fields $\longrightarrow \bar{\psi}$, ψ

gluon fields $\longrightarrow U_\mu = e^{iagA^b_\mu T_b} \in$ SU(3)

(anti-)periodic BC

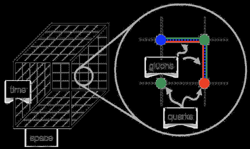

UNIFORM MAGNETIC FIELD ON THE LATTICE

fermion fields $\longrightarrow \bar{\psi}$, ψ
gluon fields $\longrightarrow U_\mu = e^{iagA_\mu^b T_b} \in$ SU(3)
magnetic field $\longrightarrow u_\mu = e^{iaqA_\mu} \in$ U(1)

(anti-)periodic BC

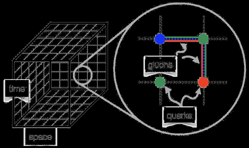

UNIFORM MAGNETIC FIELD ON THE LATTICE

fermion fields $\longrightarrow \bar{\psi}, \psi$
gluon fields $\longrightarrow U_\mu = e^{iagA_\mu^b T_b} \in$ SU(3)
magnetic field $\longrightarrow u_\mu = e^{iaqA_\mu} \in$ U(1)

$$\mathbf{B} = B\hat{z}$$

(anti-)periodic BC

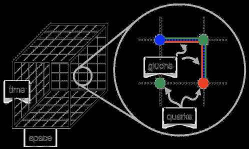

UNIFORM MAGNETIC FIELD ON THE LATTICE

fermion fields $\longrightarrow \bar{\psi}, \psi$

gluon fields $\longrightarrow U_\mu = e^{iagA_\mu^b T_b} \in$ SU(3)

magnetic field $\longrightarrow u_\mu = e^{iaqA_\mu} \in$ U(1)

(anti-)periodic BC

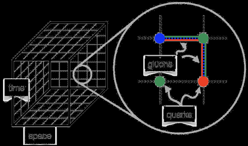

$$\mathbf{B} = B\hat{z}$$

Stoke's theorem must hold on the torus.

inner area: $\oint A_\mu dx_\mu = SB$

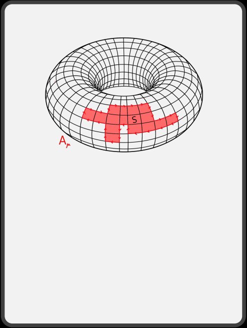

Uniform magnetic field on the lattice

fermion fields $\longrightarrow \bar{\psi}, \psi$
gluon fields $\longrightarrow U_\mu = e^{iagA_\mu^b T_b} \in$ SU(3)
magnetic field $\longrightarrow u_\mu = e^{iaqA_\mu} \in$ U(1)

$$\mathbf{B} = B\hat{z}$$

(anti-)periodic BC

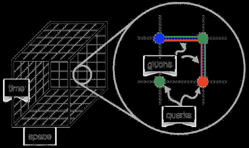

Stoke's theorem must hold on the torus.

inner area: $\oint A_\mu dx_\mu = SB$

outer area: $\oint A_\mu dx_\mu = (L_x L_y - S)B$

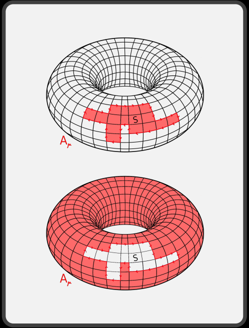

Uniform magnetic field on the lattice

fermion fields $\longrightarrow \bar{\psi}, \psi$
gluon fields $\longrightarrow U_\mu = e^{iagA_\mu^b T_b} \in$ SU(3)
magnetic field $\longrightarrow u_\mu = e^{iaqA_\mu} \in$ U(1)

$$\mathbf{B} = B\hat{z}$$

(anti-)periodic BC

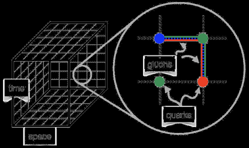

Stoke's theorem must hold on the torus.

inner area: $\oint A_\mu dx_\mu = SB$

outer area: $\oint A_\mu dx_\mu = (L_x L_y - S)B$

$$e^{-iqBS} = e^{iqB(L_x L_y - S)}$$

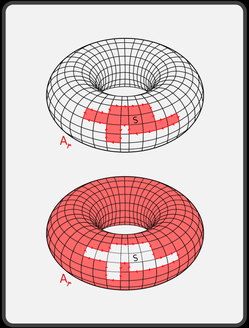

Uniform magnetic field on the lattice

fermion fields $\longrightarrow \bar{\psi}, \psi$
gluon fields $\longrightarrow U_\mu = e^{iagA_\mu^b T_b} \in$ SU(3)
magnetic field $\longrightarrow u_\mu = e^{iaqA_\mu} \in$ U(1)

$$\mathbf{B} = B\hat{z}$$

Stoke's theorem must hold on the torus.

inner area: $\oint A_\mu dx_\mu = SB$

outer area: $\oint A_\mu dx_\mu = (L_x L_y - S)B$

$$e^{-iqBS} = e^{iqB(L_x L_y - S)}$$

$$\boxed{qB = \frac{2\pi N_b}{L_x L_y}, \quad N_b \in \mathbb{Z}}$$

(anti-)periodic BC

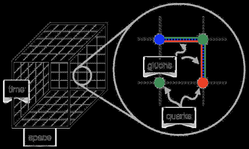

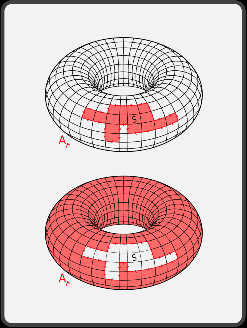

Uniform magnetic field on the lattice

$\mathbf{B} = \nabla \times \mathbf{A}$

$A_y = Bx \quad A_x = A_z = A_t = 0$

Uniform magnetic field on the lattice

$$\mathbf{B} = \nabla \times \mathbf{A}$$

$$A_y = Bx \quad A_x = A_z = A_t = 0$$

$$u_y = e^{iaqBx} \quad u_x = u_z = u_t = 1$$

Uniform magnetic field on the lattice

$$\mathbf{B} = \nabla \times \mathbf{A}$$

$$A_y = Bx \quad A_x = A_z = A_t = 0$$

$$u_y = e^{iaqBx} \quad u_x = u_z = u_t = 1$$

$$u_y(L_x) = e^{ia2\pi Nb/L_y} \neq u_y(0)$$

Uniform magnetic field on the lattice

$\mathbf{B} = \nabla \times \mathbf{A}$

$A_y = Bx \quad A_x = A_z = A_t = 0$

$u_y = e^{iaqBx} \quad u_x = u_z = u_t = 1$

$$u_y(L_x) = e^{ia2\pi Nb/L_y} \neq u_y(0)$$

We can perform gauge transformations on the links

$$u'_\mu(x) = \Omega(x) u_\mu \Omega(x + a\hat{\mu})^\dagger$$

a is the lattice spacing.

Uniform magnetic field on the lattice

$\mathbf{B} = \nabla \times \mathbf{A}$

$A_y = Bx \quad A_x = A_z = A_t = 0$

$u_y = e^{iaqBx} \quad u_x = u_z = u_t = 1$

$$u_y(L_x) = e^{ia2\pi Nb/L_y} \neq u_y(0)$$

We can perform gauge transformations on the links

$$u'_\mu(x) = \Omega(x) u_\mu \Omega(x + a\hat{\mu})^\dagger$$

a is the lattice spacing.

$$u_x = \begin{cases} e^{-iqBL_x y} & \text{if } x = L_x - a \\ 1 & \text{if } x \neq L_x - a \end{cases}$$

$$u_y = e^{iaqBx} \quad 0 \leq x \leq L_x - a$$

$$u_z = 1$$

$$u_t = 1$$

Inhomogeneous magnetic field on the lattice

INHOMOGENEOUS MAGNETIC FIELD ON THE LATTICE

$$\mathbf{B} = \frac{B}{\cosh\left(\frac{x - L_x/2}{\epsilon}\right)^2}\hat{z}$$

Profile motivated by heavy-ion collision scenarios Deng and Huang 2012, Cao 2018.

Inhomogeneous magnetic field on the lattice

$$\mathbf{B} = \frac{B}{\cosh\left(\frac{x - L_x/2}{\epsilon}\right)^2}\hat{z}$$

Profile motivated by heavy-ion collision scenarios Deng and Huang 2012, Cao 2018.

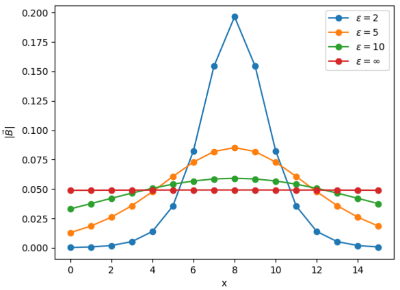

INHOMOGENEOUS MAGNETIC FIELD ON THE LATTICE

$$\mathbf{B} = \frac{B}{\cosh\left(\frac{x - L_x/2}{\epsilon}\right)^2}\hat{z}$$

Profile motivated by heavy-ion collision scenarios Deng and Huang 2012, Cao 2018.

$$qB = \frac{\pi N_b}{L_y \epsilon \tanh\left(\frac{L_x}{2\epsilon}\right)} \qquad N_b \in \mathbb{Z}$$

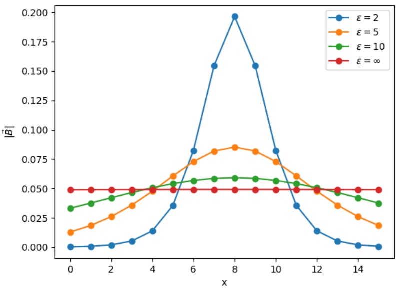

INHOMOGENEOUS MAGNETIC FIELD ON THE LATTICE

$$\mathbf{B} = \frac{B}{\cosh\left(\frac{x-L_x/2}{\epsilon}\right)^2}\hat{z}$$

Profile motivated by heavy-ion collision scenarios Deng and Huang 2012, Cao 2018.

$$qB = \frac{\pi N_b}{L_y \epsilon \tanh\left(\frac{L_x}{2\epsilon}\right)} \qquad N_b \in \mathbb{Z}$$

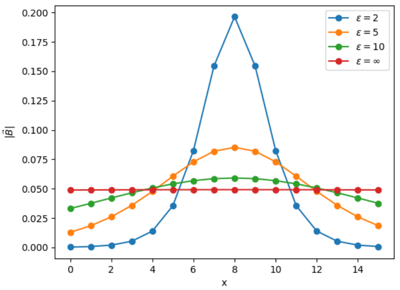

$$u_x = \begin{cases} e^{-2iqB\epsilon y \tanh\left(\frac{L_x}{2\epsilon}\right)} & \text{if } x = L_x - a \\ 1 & \text{if } x \neq L_x - a \end{cases}$$

$$u_y = e^{iaqB\epsilon\left[\tanh\left(\frac{x-L_x/2}{\epsilon}\right)+\tanh\left(\frac{L_x}{2\epsilon}\right)\right]}, \quad 0 \leq x \leq L_x - a$$

$$u_z = u_t = 1$$

Lattice simulations

THE SIMULATION SET UP

THE SIMULATION SET UP

- Improved staggered fermions with $N_f = 2 + 1$ flavors and physical masses;

THE SIMULATION SET UP

- Improved staggered fermions with $N_f = 2 + 1$ flavors and physical masses;
- Lattices: $16^3 \times 6 \quad 24^3 \times 8 \quad 28^3 \times 10 \quad 36^3 \times 12 \quad \longrightarrow$ continuum limit (lattice spacing $\to 0$, $V =$ const.);

The simulation set up

- Improved staggered fermions with $N_f = 2 + 1$ flavors and physical masses;
- Lattices: $16^3 \times 6 \quad 24^3 \times 8 \quad 28^3 \times 10 \quad 36^3 \times 12 \quad \longrightarrow$ continuum limit (lattice spacing $\to 0$, $V =$ const.);
- Number of gauge confiigurations $\sim \mathcal{O}(200)$ - $\mathcal{O}(700)$;

THE SIMULATION SET UP

- Improved staggered fermions with $N_f = 2+1$ flavors and physical masses;
- Lattices: $16^3 \times 6 \quad 24^3 \times 8 \quad 28^3 \times 10 \quad 36^3 \times 12 \quad \longrightarrow$ continuum limit (lattice spacing $\to 0$, $V =$ const.);
- Number of gauge confiigurations $\sim \mathcal{O}(200)$ - $\mathcal{O}(700)$;
- Magnetic field

$$\mathbf{B} = \frac{B}{\cosh\left(\dfrac{x - L_x/2}{\epsilon}\right)^2}\hat{z} \qquad eB = \frac{3\pi N_b}{L_y \epsilon \tanh\left(\frac{L_x}{2\epsilon}\right)} \qquad \epsilon \approx 0.6 \text{ fm}$$

strength 0 GeV $\leq \sqrt{eB} \leq 1.2$ GeV;

THE SIMULATION SET UP

- Improved staggered fermions with $N_f = 2+1$ flavors and physical masses;
- Lattices: $16^3 \times 6 \quad 24^3 \times 8 \quad 28^3 \times 10 \quad 36^3 \times 12 \quad \longrightarrow$ continuum limit (lattice spacing $\to 0$, $V =$ const.);
- Number of gauge confiigurations $\sim \mathcal{O}(200)$ - $\mathcal{O}(700)$;
- Magnetic field

$$\mathbf{B} = \frac{B}{\cosh\left(\frac{x - L_x/2}{\epsilon}\right)^2}\hat{z} \qquad eB = \frac{3\pi N_b}{L_y \epsilon \tanh\left(\frac{L_x}{2\epsilon}\right)} \qquad \epsilon \approx 0.6 \text{ fm}$$

strength 0 GeV $\leq \sqrt{eB} \leq 1.2$ GeV;

- Temperature range 68 MeV $\leq T \leq 300$ MeV (crossover transition at $T_c \sim 155$ MeV).

Lattice observables

LATTICE OBSERVABLES

- Local chiral condensates (**u** and **d** quarks!)

$\bar{\psi}\psi$

Lattice observables

- Local chiral condensates (u and d quarks!)

$$\bar{\psi}\psi \quad \xrightarrow{\text{renormalization}} \quad \Sigma(x,T,B) = \frac{m_{ud}}{m_\pi^4}\left[\bar{\psi}\psi(x,T,B) - \bar{\psi}\psi(x,T,0)\right]$$

LATTICE OBSERVABLES

- Local chiral condensates (u and d quarks!)

$$\bar{\psi}\psi \xrightarrow{\text{renormalization}} \Sigma(x,T,B) = \frac{m_{ud}}{m_\pi^4}\left[\bar{\psi}\psi(x,T,B) - \bar{\psi}\psi(x,T,0)\right]$$

- Local Polyakov loop

$$P = \frac{1}{L_x L_y}\sum_{y,z} \mathrm{Re}\,\mathrm{Tr}\prod_n U_t(x,y,z,n)$$

Lattice observables

- Local chiral condensates (u and d quarks!)

$$\bar\psi\psi \xrightarrow{\text{renormalization}} \Sigma(x,T,B) = \frac{m_{ud}}{m_\pi^4}\left[\bar\psi\psi(x,T,B) - \bar\psi\psi(x,T,0)\right]$$

- Local Polyakov loop

$$P = \frac{1}{L_x L_y}\sum_{y,z} \mathrm{Re}\,\mathrm{Tr}\prod_n U_t(x,y,z,n) \xrightarrow{\text{renormalization}} \frac{P(x,T,B)}{P(x,T,0)}$$

LATTICE OBSERVABLES

- Local chiral condensates (u and d quarks!)

$$\bar{\psi}\psi \xrightarrow{\text{renormalization}} \Sigma(x,T,B) = \frac{m_{ud}}{m_\pi^4}\left[\bar{\psi}\psi(x,T,B) - \bar{\psi}\psi(x,T,0)\right]$$

- Local Polyakov loop

$$P = \frac{1}{L_x L_y}\sum_{y,z} \mathrm{Re}\,\mathrm{Tr}\prod_n U_t(x,y,z,n) \xrightarrow{\text{renormalization}} \frac{P(x,T,B)}{P(x,T,0)}$$

- Local electric currents (u, d and s quarks!)

$$\langle\, J_i(x)\,\rangle = e\left\langle\, \frac{2}{3}\bar{u}\gamma^i u - \frac{1}{3}\bar{d}\gamma^i d - \frac{1}{3}\bar{s}\gamma^i s \,\right\rangle$$

CHIRAL CONDENSATE - $\Sigma(T,B) = \frac{m_{ud}}{m_\pi^4}[\bar{\psi}\psi(T,B) - \bar{\psi}\psi(T,0)]$

CHIRAL CONDENSATE - $\Sigma(T,B) = \frac{m_{ud}}{m_\pi^4}[\bar{\psi}\psi(T,B) - \bar{\psi}\psi(T,0)]$

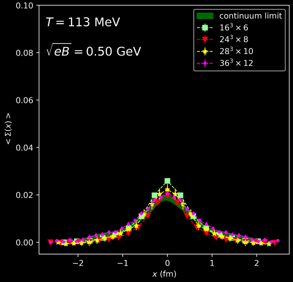

CHIRAL CONDENSATE - $\Sigma(T,B) = \frac{m_{ud}}{m_\pi^4}[\bar{\psi}\psi(T,B) - \bar{\psi}\psi(T,0)]$

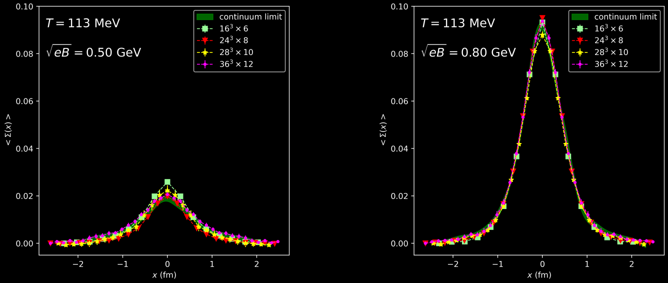

Chiral condensate - $\Sigma(T,B) = \frac{m_{ud}}{m_\pi^4}[\bar\psi\psi(T,B) - \bar\psi\psi(T,0)]$

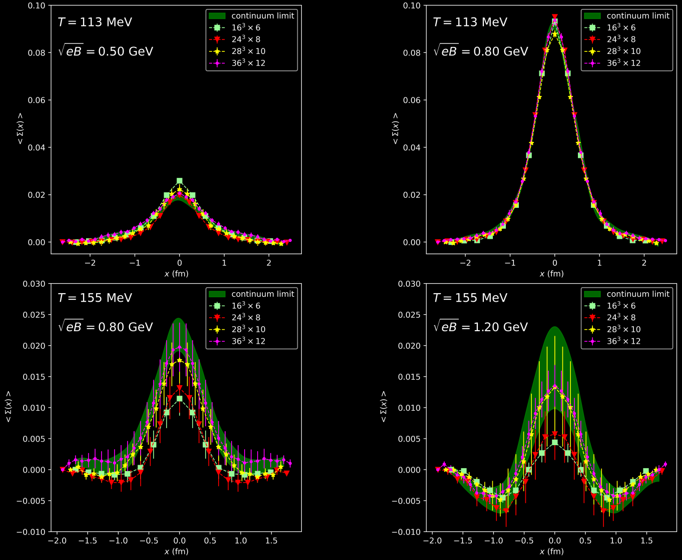

Chiral condensate - $\Sigma(T,B) = \frac{m_{ud}}{m_\pi^4}[\bar{\psi}\psi(T,B) - \bar{\psi}\psi(T,0)]$

What happens to the peak of the condensate as a function of T and B?

CHIRAL CONDENSATE - $\Sigma(T,B) = \frac{m_{ud}}{m_\pi^4}[\bar{\psi}\psi(T,B) - \bar{\psi}\psi(T,0)]$

What happens to the peak of the condensate as a function of T and B?

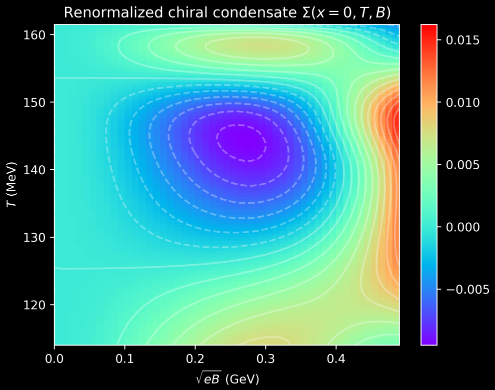

- Magnetic catalysis T away from Tc

CHIRAL CONDENSATE - $\Sigma(T,B) = \frac{m_{ud}}{m_\pi^4}[\bar{\psi}\psi(T,B) - \bar{\psi}\psi(T,0)]$

What happens to the peak of the condensate as a function of T and B?

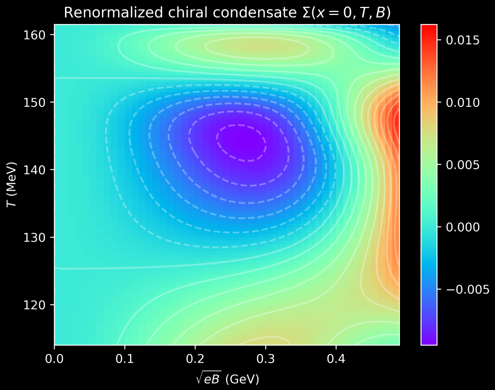

- Magnetic catalysis T away from Tc
- Inverse catalysis for T around T_c Endrődi et al. 2019

POLYAKOV LOOP - $P(x,T,B)/P(x,T,0)$

POLYAKOV LOOP - $P(x,T,B)/P(x,T,0)$

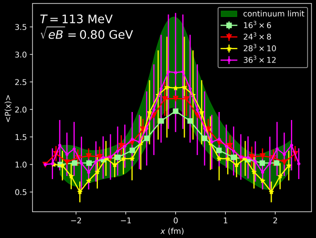

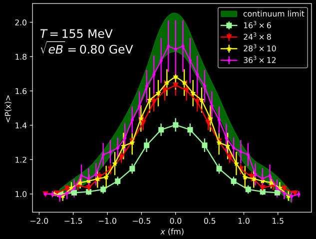

POLYAKOV LOOP - $P(x,T,B)/P(x,T,0)$

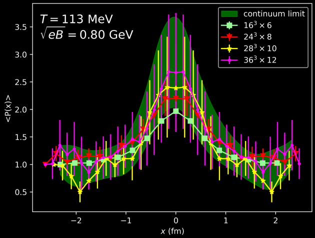

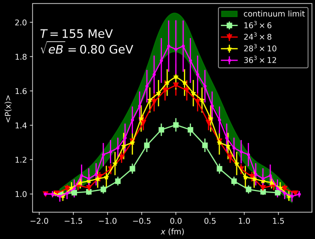

The Polyakov loop is typically broader than the chiral condensate.

POLYAKOV LOOP - $P(x,T,B)/P(x,T,0)$

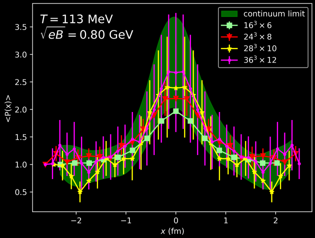

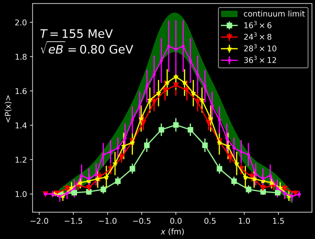

The Polyakov loop is typically broader than the chiral condensate.

$$\langle\ \bar{\psi}\psi(x)P(y)\ \rangle - \langle\ \bar{\psi}\psi(x)\ \rangle\langle\ P(x)\ \rangle$$

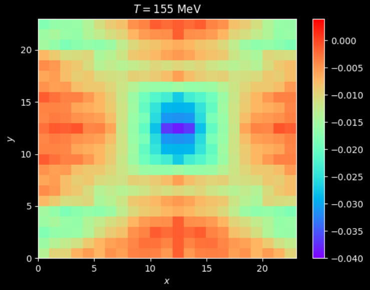

Polyakov loop - $P(x,T,B)/P(x,T,0)$

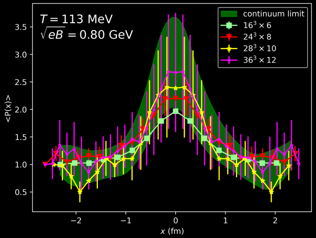

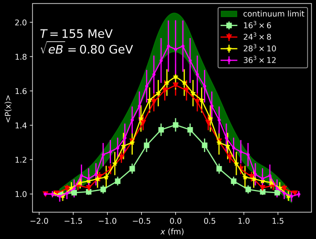

The Polyakov loop is typically broader than the chiral condensate.

$$\langle\, \bar\psi\psi(x)P(y)\,\rangle - \langle\, \bar\psi\psi(x)\,\rangle\langle\, P(x)\,\rangle$$

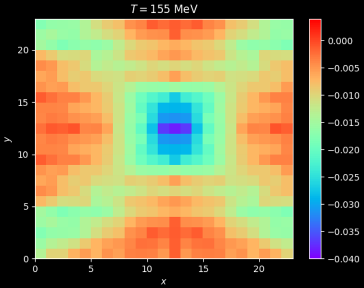

The interaction of the condensate with P causes the dips!

Electric currents - $J^i = \sum_f \frac{q_f}{e}\bar{\psi}_f\gamma^i\psi_f$

ELECTRIC CURRENTS - $J^i = \sum_f \frac{q_f}{e}\bar{\psi}_f\gamma^i\psi_f$

$\mathbf{J} \sim \boldsymbol{\nabla} \times \mathbf{B}$

ELECTRIC CURRENTS - $J^i = \sum_f \frac{q_f}{e}\bar{\psi}_f\gamma^i\psi_f$

$$\mathbf{J} \sim \nabla \times \mathbf{B} \quad \longrightarrow \quad J_y \sim \frac{\partial B_z}{\partial x}$$

ELECTRIC CURRENTS - $J^i = \sum_f \frac{q_f}{e}\bar{\psi}_f\gamma^i\psi_f$

$$\mathbf{J} \sim \nabla \times \mathbf{B} \quad \longrightarrow \quad J_y \sim \frac{\partial B_z}{\partial x} = -\frac{2B}{\epsilon \cosh\left(\frac{x - L_x/2}{\epsilon}\right)^2} \tanh\left(\frac{x - L_x/2}{\epsilon}\right)$$

ELECTRIC CURRENTS - $J^i = \sum_f \frac{q_f}{e} \bar{\psi}_f \gamma^i \psi_f$

$$\mathbf{J} \sim \nabla \times \mathbf{B} \quad \longrightarrow \quad J_y \sim \frac{\partial B_z}{\partial x} = -\frac{2B}{\epsilon \cosh\left(\frac{x - L_x/2}{\epsilon}\right)^2} \tanh\left(\frac{x - L_x/2}{\epsilon}\right)$$

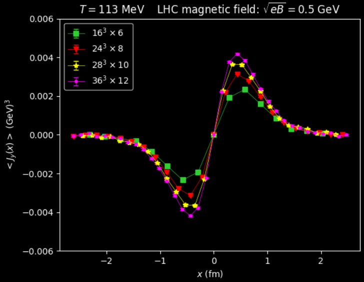

ELECTRIC CURRENTS - $J^i = \sum_f \frac{q_f}{e}\bar{\psi}_f\gamma^i\psi_f$

$$\mathbf{J} \sim \nabla \times \mathbf{B} \quad \longrightarrow \quad J_y \sim \frac{\partial B_z}{\partial x} = -\frac{2B}{\epsilon\cosh\left(\frac{x-L_x/2}{\epsilon}\right)^2}\tanh\left(\frac{x-L_x/2}{\epsilon}\right)$$

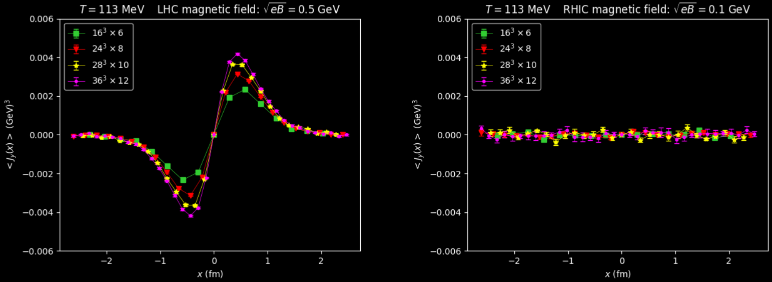

Figure 6: Lattice electric currents for LHC-like ($\sqrt{eB} = 0.5$ GeV) and RHIC-like ($\sqrt{eB} = 0.1$ GeV) magnetic fields, respectively.

(Bare) magnetic susceptibility

(Bare) magnetic susceptibility

$$\frac{1}{\mu_0}\mathbf{B} = \mathbf{H} + \mathbf{M} \quad \longrightarrow \quad \mathbf{J}_{tot} = \mathbf{J}_f + \mathbf{J}_m \quad \longrightarrow \quad \mathbf{J}_m = \boldsymbol{\nabla} \times \mathbf{M}$$

(Bare) magnetic susceptibility

$$\frac{1}{\mu_0}\mathbf{B} = \mathbf{H} + \mathbf{M} \quad \longrightarrow \quad \mathbf{J}_{tot} = \mathbf{J}_f + \mathbf{J}_m \quad \longrightarrow \quad \mathbf{J}_m = \boldsymbol{\nabla} \times \mathbf{M}$$

- Linear medium:
  $\mathbf{M} \approx \chi_m \mathbf{H}$

(Bare) magnetic susceptibility

$$\frac{1}{\mu_0}\mathbf{B} = \mathbf{H} + \mathbf{M} \quad \longrightarrow \quad \mathbf{J}_{tot} = \mathbf{J}_f + \mathbf{J}_m \quad \longrightarrow \quad \mathbf{J}_m = \nabla \times \mathbf{M}$$

- Linear medium:
  $\mathbf{M} \approx \chi_m \mathbf{H}$
- $\dfrac{\chi_m}{1+\chi_m}\nabla \times \mathbf{B} = \mathbf{J}_m$

(BARE) MAGNETIC SUSCEPTIBILITY

$$\frac{1}{\mu_0}\mathbf{B} = \mathbf{H} + \mathbf{M} \quad \longrightarrow \quad \mathbf{J}_{tot} = \mathbf{J}_f + \mathbf{J}_m \quad \longrightarrow \quad \mathbf{J}_m = \nabla \times \mathbf{M}$$

- Linear medium:
  $\mathbf{M} \approx \chi_m \mathbf{H}$
- $\dfrac{\chi_m}{1+\chi_m}\nabla \times \mathbf{B} = \mathbf{J}_m$

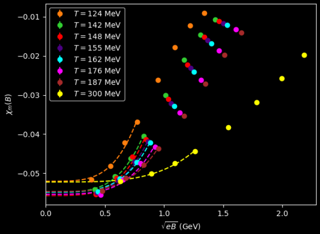

(BARE) MAGNETIC SUSCEPTIBILITY

$$\frac{1}{\mu_0}\mathbf{B} = \mathbf{H} + \mathbf{M} \longrightarrow \mathbf{J}_{tot} = \mathbf{J}_f + \mathbf{J}_m \longrightarrow \mathbf{J}_m = \nabla \times \mathbf{M}$$

- Linear medium: $\mathbf{M} \approx \chi_m \mathbf{H}$
- $\frac{\chi_m}{1+\chi_m} \nabla \times \mathbf{B} = \mathbf{J}_m$

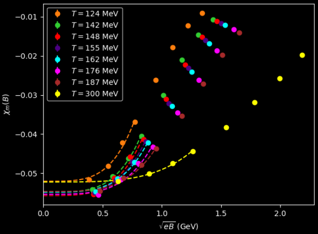

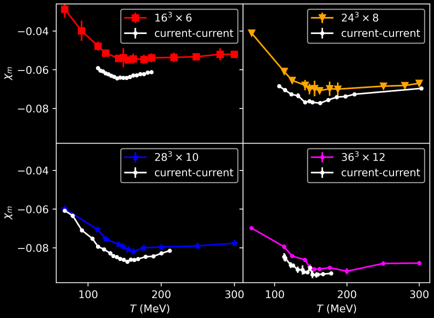

(BARE) MAGNETIC SUSCEPTIBILITY

$$\frac{1}{\mu_0}\mathbf{B} = \mathbf{H} + \mathbf{M} \quad \longrightarrow \quad \mathbf{J}_{tot} = \mathbf{J}_f + \mathbf{J}_m \quad \longrightarrow \quad \mathbf{J}_m = \nabla \times \mathbf{M}$$

- Linear medium: $\mathbf{M} \approx \chi_m \mathbf{H}$
- $\dfrac{\chi_m}{1+\chi_m} \nabla \times \mathbf{B} = \mathbf{J}_m$

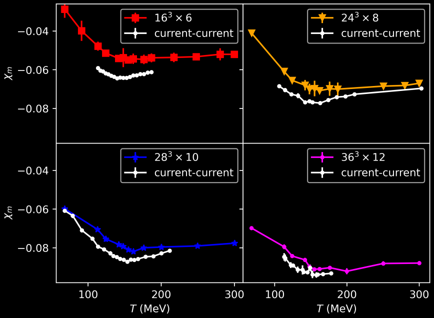

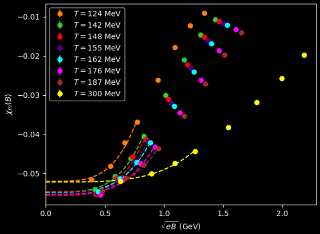

The susceptibility contains an additive divergence $\chi_m \sim \log(a)$

(Renormalized) magnetic susceptibility

The divergence is independent of T: $\chi_m^r(T) \equiv \chi_m(T) - \chi_m(0)$

(Renormalized) magnetic susceptibility

The divergence is independent of T: $\chi_m^r(T) \equiv \chi_m(T) - \chi_m(0)$

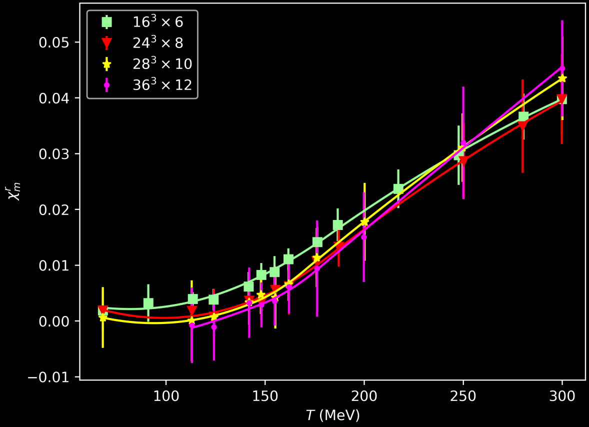

(Renormalized) magnetic susceptibility

The divergence is independent of T: $\chi_m^r(T) \equiv \chi_m(T) - \chi_m(0)$

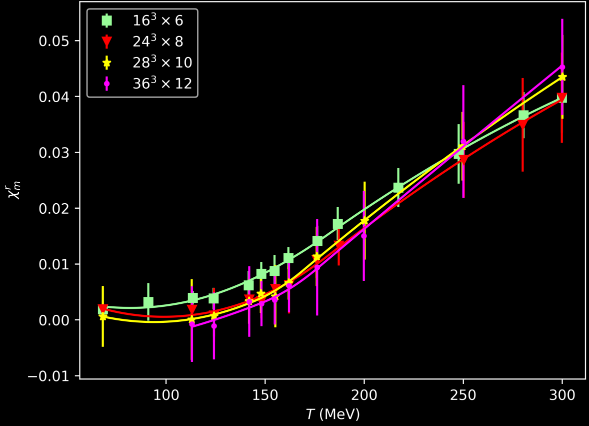

- $\chi_m^r < 0$: diamagnetism
- $\chi_m^r > 0$: paramagnetism

(Renormalized) magnetic susceptibility

The divergence is independent of T: $\chi_m^r(T) \equiv \chi_m(T) - \chi_m(0)$

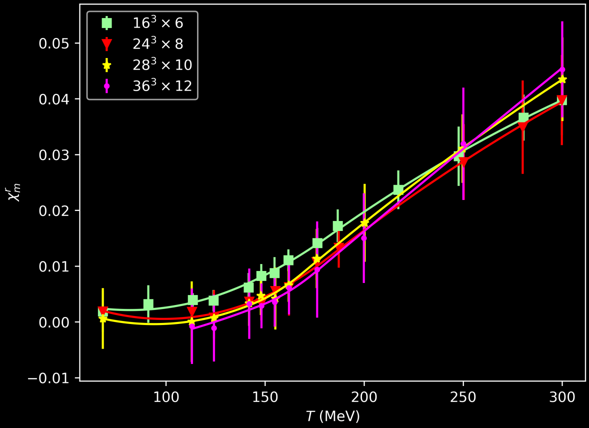

- $\chi_m^r < 0$: diamagnetism
- $\chi_m^r > 0$: paramagnetism

Great agreement with the current-current method! Bali, Gergely Endrődi, and Piemonte 2020

Summary & Conclusions

Summary & Conclusions

- A richer scenario emerges in the presence of an inhomogeneous B (dips, steady eletric currents, etc.);

Summary & Conclusions

- A richer scenario emerges in the presence of an inhomogeneous B (dips, steady eletric currents, etc.);
- Electric currents are prominent for LHC-like magnetic fields and stronger;

Summary & Conclusions

- A richer scenario emerges in the presence of an inhomogeneous B (dips, steady eletric currents, etc.);
- Electric currents are prominent for LHC-like magnetic fields and stronger;
- Using J_m and Maxwell's equations we introduced a new method to compute χ_m;

Summary & Conclusions

- A richer scenario emerges in the presence of an inhomogeneous B (dips, steady eletric currents, etc.);
- Electric currents are prominent for LHC-like magnetic fields and stronger;
- Using J_m and Maxwell's equations we introduced a new method to compute χ_m;
- Our χ_m corroborates the picture of weak diamagnetism in QCD for $T < T_c$ and strong paramagnetism for $T > T_c$;

Summary & Conclusions

- A richer scenario emerges in the presence of an inhomogeneous B (dips, steady eletric currents, etc.);
- Electric currents are prominent for LHC-like magnetic fields and stronger;
- Using J_m and Maxwell's equations we introduced a new method to compute χ_m;
- Our χ_m corroborates the picture of weak diamagnetism in QCD for $T < T_c$ and strong paramagnetism for $T > T_c$;
- The knowledge of these processes is important to capture the correct physics in heavy-ion collision studies (QCD models, hydrodynamics, etc.);

Summary & Conclusions

- A richer scenario emerges in the presence of an inhomogeneous B (dips, steady eletric currents, etc.);
- Electric currents are prominent for LHC-like magnetic fields and stronger;
- Using J_m and Maxwell's equations we introduced a new method to compute χ_m;
- Our χ_m corroborates the picture of weak diamagnetism in QCD for $T < T_c$ and strong paramagnetism for $T > T_c$;
- The knowledge of these processes is important to capture the correct physics in heavy-ion collision studies (QCD models, hydrodynamics, etc.);
- More on electromagnetic fields in lattice QCD: posters by

J. J. H. Hernandez

E. Garnacho Velasco

Bibliography I

References

Deng, Wei-Tian and Xu-Guang Huang (2012). "Event-by-event generation of electromagnetic fields in heavy-ion collisions". In: *Physical Review C* 85.4, p. 044907.

Cao, Gaoqing (2018). "Chiral symmetry breaking in a semilocalized magnetic field". In: *Physical Review D* 97.5, p. 054021.

Endrődi, G et al. (2019). "Magnetic catalysis and inverse catalysis for heavy pions". In: *Journal of High Energy Physics* 2019.7, pp. 1–15.

Bibliography II

Bali, Gunnar S, Gergely Endrődi, and Stefano Piemonte (2020). "Magnetic susceptibility of QCD matter and its decomposition from the lattice". In: *Journal of High Energy Physics* 2020.7, pp. 1–43.